Tikrit Journal of Engineering Sciences (2025); 32(1): 1306
DOI: http://doi.org/10.25130/tjes.32.1.10

IRAQI Academic Scientific Journals

ISSN: 1813-162X (Print); 2312-7589 (Online)
Tikrit Journal of Engineering Sciences
available online at: http://www.tj-es.com

TJES Tikrit Journal of Engineering Sciences

Air Pollution Dispersion Modeling from Point Sources Using Gaussian Plume Model: A Case Study of Kirkuk, Iraq

Ahmed Saeed Salih *, Nihad Davut Hassan, Nada Subhi Abdulmajeed
Department of Surveying Engineering Techniques, Technical College of Kirkuk, Northern Technical University, Kirkuk, Iraq.

Keywords:
Air pollution; Gaussian plume model; GIS; Point source emissions; Remote sensing.

Highlights:

- *Simulated pollutant dispersion from an oil refinery in Kirkuk, Iraq, using the Gaussian plume model to understand concentration patterns.*
- *Evaluated the influence of wind speed, wind direction, and pollutant type on dispersion patterns and concentration levels.*
- *CO and CO2 exhibited higher concentrations compared to particulate matter.*

ARTICLE INFO
Article history:

Received	08 July	2023
Received in revised form	25 July	2023
Accepted	26 Jan.	2024
Final Proofreading	20 Nov.	2024
Available online	20 Mar.	2025

Citation: Salih AS, Hassan ND, Abdulmajeed NS. **Air Pollution Dispersion Modeling from Point Sources using Gaussian Plume Model: A Case Study of Kirkuk, Iraq**. *Tikrit Journal of Engineering Sciences* 2025; **32**(1): 1306.
http://doi.org/10.25130/tjes.32.1.10

*Corresponding author:

Ahmed Saeed Salih
Department of Surveying Engineering Techniques, Technical College of Kirkuk, Northern Technical University, Kirkuk, Iraq.

Abstract: The present study models the dispersion of air pollutants from Kirkuk Oil Refinery to Kirkuk City. The study considers the impact of pollution type, wind speed, and wind direction on the dispersion patterns. The simulated pollutants concentrations were in µg/m³ to provide valuable knowledge of the pollution levels. The Gaussian plume model was used to simulate various pollutants' air pollution concentrations produced by the refinery. The results showed a wide concentration range, i.e., from 1.19×10^{-28} µg/m³ to 11.26 µg/m³. The mean concentration was 0.46 µg/m³. Different wind directions caused a minimum concentration of 0 µg/m³, i.e., negligible or low pollution levels away from the emission source. The mean concentration slightly varied with the wind direction, i.e., from 8.37×10^{-3} to 8.56×10^{-3} µg/m³. In other words, the mean pollution levels remained adequately low regardless of the wind direction. On the other hand, the wind direction impacted the maximum concentration. At 235°, the highest maximum concentration was 23.807 µg/m³, and at 174°, the lowest maximum concentration was 9.28569 µg/m³. Also, the results regarding the pollutant revealed that Co2 showed the highest mean concentration, i.e., 5.321 µg/m³, and the highest maximum concentration, i.e., 6734.623 µg/m³. Gases, e.g., Co, No2, and So2, showed higher concentrations than PM1, PM2.5, PM5, and PM10, implying that atmospheric behavior and emission sources differ. These results expand understanding of the air pollution dispersion patterns and provide a clear vision for policymakers and environmental managers. Future works should focus on refining modeling approaches and utilizing real-time data to obtain accurate pollutant dispersion pattern predictions.

نمذجة تشتت تلوث الهواء من مصادر نقطية باستخدام نموذج السحابة الجاوسية: منطقة الدراسة كركوك، العراق

احمد سعيد صالح، نهاد داوود حسن، ندى صبحي عبد المجيد
قسم تقنيات هندسة المساحة/ الكلية التقنية كركوك/ الجامعة التقنية الشمالية / كركوك – العراق.

الخلاصة

الهدف الرئيسي لهذه الدراسة هو نمذجة تشتت ملوثات الهواء من مصفاة نفط كركوك إلى المدينة، مع التركيز بشكل خاص على تحديد كيفية تأثير نوع التلوث وسرعة الرياح واتجاه الرياح على أنماط التشتت. يتم قياس تركيز المحاكاة للملوثات كمياً بالميكروجرام لكل متر مكعب (ميكروغرام / م ٣)، مما يوفر رؤى قيمة حول مستويات التلوث عبر منطقة الدراسة. يتم استخدام نموذج السحابة الجاوسية لمحاكاة تركيزات تلوث الهواء للعديد من الملوثات المنبعثة من المصفاة. تشير النتائج الرئيسية إلى مدى واسع من التركيزات، بحد أدنى للتركيز ١,١٩e-28 ميكروغرام / م ٣، وأقصى تركيز ١١,٢٦ ميكروغرام / م ٣، ومتوسط تركيز ٠,٤٦ ميكروغرام / م ٣. يكشف تحليل البيانات عبر اتجاهات الرياح المختلفة عن تركيزات دنيا متسقة تبلغ ٠ ميكروغرام / متر مكعب، مما يشير إلى مستويات تلوث منخفضة أو لا تذكر في المناطق البعيدة من نقطة المصدر. تختلف التركيزات المتوسطة قليلاً مع اتجاه الرياح، وتتراوح من ٠,٠٠٨٣٧ ميكروغرام / متر مكعب إلى ٠,٠٠٨٥٦ ميكروغرام / متر مكعب. يشير هذا إلى أن متوسط مستويات التلوث لا يزال منخفضًا نسبيًا بغض النظر عن اتجاه الرياح. ومع ذلك، تظهر التركيزات القصوى اختلافات بناءً على اتجاه الرياح، حيث سجلت أعلى مستوياتها عند ٢٣,٨٠٧ ميكروغرام / متر مكعب لاتجاه رياح يبلغ ٢٣٥ درجة وأدنىها عند ٩,٢٨٥٦٩ ميكروغرام / متر مكعب لاتجاه الرياح بمقدار ١٧٤ درجة. هذا يسلط الضوء على تأثير اتجاه الرياح على تركيزات الملوثات في مناطق محددة في اتجاه الريح. بالإضافة إلى ذلك، أظهرت مستويات التركيز لكل ملوث، حيث أظهر ثاني أكسيد الكربون أعلى متوسط تركيز قدره ٥,٣٢١ ميكروغرام / متر مكعب وأعلى تركيز أقصى قدره ٦٧٣٤,٦٢٣ ميكروغرام / متر مكعب. تظهر غازات مثل ثاني أكسيد الكربون وثاني أكسيد الكبريت وثاني أكسيد النيتروجين تركيزات أعلى نسبيًا مقارنة بملوثات الجسيمات (PM_1 و $PM_{2.5}$ و PM_5 و PM_{10})، مما يعكس الاختلافات في مصادر الانبعاث وسلوك الغلاف الجوي. تساهم هذه النتائج في فهم أنماط تشتت تلوث الهواء وتوفر رؤى قيمة للإدارة البيئية وصنع السياسات. يجب أن تركز الأبحاث المستقبلية على تحسين تقنيات النمذجة ودمج البيانات في الوقت الفعلي للحصول على تنبؤات أكثر دقة لأنماط تشتت الملوثات.

الكلمات الدالة: انبعاثات المصدر النقطي، الاستشعار عن بعد، تلوث الهواء، نظم المعلومات الجغرافية، نموذج السحابة الجاوسية.

1.INTRODUCTION

Air quality is a vital environmental issue. Urban, industrial, and transportation emissions worsen this issue. Major cities in Iraq suffer from high pollution levels due to outdated infrastructure, rapid urban growth, and conflicts. Air pollution is a vital issue in Kirkuk City-Iraq because it contains many refineries emitting massive pollutants into the air, including nitrogen oxides, sulfur dioxide, and volatile organic compounds. Such pollutants cause many health issues, e.g., respiratory disorders, heart disease, and cancer. Surrounding areas of Kirkuk City are also impacted by pollutants, causing human and environmental issues [1]. Studying air pollution dispersion from its source is significant in evaluating health risks, developing air quality regulations, and designing effective mitigation strategies. Understanding how pollutants disperse from their sources helps estimate the potential risks impacting human health and the environment. The pollutant type, the height of the emission source, wind speed, and terrain impact the pollution dispersion. Understanding these parameters enables highly trusted decisions to reduce risks and enhance air quality. The Gaussian plume model predicts the dispersion of air pollution from its source. The model assumes that pollutants follow the Gaussian profile while the wind speed and direction are constant, which limits this model despite being cost-effective and simple. However, it is useful for air pollution planning, control device design, and predicting accidental releases. The accuracy depends on pollutant type, emission source height, wind characteristics, and terrain [2]. Khan and Hassan [3] reviewed air quality modeling, focusing on dispersion modeling. They discussed developing simple Gaussian plume models and more advanced models that consider the atmosphere properties, including Gaussian, Eulerian, Lagrangian, and advanced dispersion models. These models were compared based on their characteristic features. Moharreri et al. [4] assessed the exposure levels of PM_{10} and carbon monoxide (CO) from four power plants in Mashhad, Iran, using an air pollution dispersion model. The results indicated that pollutants from the power plants can be transported over long distances and significantly impact the residents' health. More recently, Saleh and Hassoon [5] studied the relationship between CO emissions from different fuels in a refinery and atmospheric stability. The study quantitatively analyzed the concentrations of CO pollutants at various distances from the emission source. It was found that during January and July, concentrations in stability classes B and F were significantly higher, reaching 120% to 170% compared to other classes (C, D, and G) that decreased by 81% to 59% with distance (1000 m-10000 m). Classes A and E differed between the two months. Furthermore, Atamaleki et al. [6] examined the effects of three phases of the Bonjourd cement factory's development on CO, SO_2, NO_x, and PM_{10} emissions. Box models are the simplest computational models that can be used to estimate the dispersion of air pollution in the atmosphere [7]. The AUSTAL 2000 model was used to analyze emission data collected over 19 years. The results showed that the second period of development had the greatest emission rate per unit area for PM_{10} and SO_2; however, a bag filter in the third

period significantly reduced their concentrations to the levels of the first period. However, NO_x and CO emissions increased the second and third times. In another paper, researchers focused on quantifying the emissions of methane from landfills using the Tracer Dispersion Method (TDM) and a Gaussian dispersion model (AERMOD) [8]. The findings revealed that when full mixing conditions were satisfied at ground level, variations in mixing higher up introduced an error of less than 10%. In Sheffield, United Kingdom, the Airviro air quality dispersion modeling tool was employed to monitor and model the air pollutants nitrogen oxides (NO_x) and particulate matter (PM_{10}) [9]. The results suggested three NO_x hotspots, including Sheffield City Centre, Darnall, and Tinsley Roundabout, while high PM_{10} concentrations were observed between Sheffield Forgemasters International and Meadow Hall Shopping Centre. Road traffic mainly contributed to NO_x, whereas point sources influenced PM_{10} levels.
Moreover, a study validated and enhanced the Gaussian plume model to predict the dispersion of ammonia and particulate matter (PM) emissions from ventilation duct fans in poultry houses [10]. The modified model incorporated a virtual source point of emissions behind the exhaust duct fan. Validation using field measurements showed significantly improved prediction accuracy, with a higher percentage of correct predictions within a factor of two (FAC_2) for both ammonia and PM than the original model. Another research focused on quantifying nitrogen dioxide (NO_2) emissions from the Durra refinery and its impact on the surrounding area [11]. A Gaussian model implemented through the MATLAB program considered wind direction, stability, and stack height. The results indicated that the most affected areas, Al-Jadriyah and Al-Karada, located 3-5 km from the refinery, experience NO_2 concentrations exceeding national air quality standards. The study analyzed 38 relevant studies that applied machine learning techniques from the past six years [12]. The research aimed to understand the fundamentals of machine learning and its function in enhancing forecast performance for atmospheric pollutant concentrations. The study examined the impact of input predictors, the geographical distribution of the studies, techniques used for estimation or forecasting, and the choice of algorithms (Neural Network, Linear Regression, Ensemble learning, or Support Vector Machine). According to the findings, machine-learning techniques were predominantly used in America and Europe. Additionally, the analysis showed that pollution estimation often relied on linear regression approaches and ensemble learning while forecasting tasks commonly employed support vector machines and neural networks. Air pollution was evaluated in the East Baghdad oil field using the ICP-MS technique [13]. The analysis revealed that the Total Suspended Particles (TSP) air load exceeded the Iraqi and the World Health Organization allowable limits standards. The average CO, CO_2, and SO_2 concentrations were within national and international standards; however, NO_2 exceeded the limits. The air quality in the area was deemed good for CO, CO_2, and NO_2 with no health effects, except hazardous for TSP, posing a significant risk to individuals with respiratory conditions. The concentrations of Cd, Cr, Cu, and Co were also higher than the prescribed limits, attributed to the oil field's operational processes and crude oil combustion, while Ni concentration remained within the limits. Another study reviewed integrating green infrastructure (GI) in dispersion models to assess its influence on health risk assessment and air pollutant concentrations [14]. The analysis examined the deposition velocities and dataset parameterization required for deposition schemes on different spatial scales. The study found that a detailed representation of GI impacts in dispersion models was complex and resource-intensive. However, the i-Tree tool and the BenMap model were combined to assess the health effects of air pollution reduction through green infrastructure canopies. The study highlighted the need for further research on short-term exposure changes, pollutant concentration redistribution, and enhanced atmospheric pollutant dilution due to GI. On the other hand, a study reviewed air pollution in various Iraqi regions [15]. It reviewed previous studies conducted in Iraq and identified various gaseous pollutants, including CO, CO_2, NO_x, SO_x, O_3, suspended particles, polycyclic aromatic hydrocarbons, and heavy metals. Ref. [15] reported that the key pollution sources are industry, energy production, fossil fuel, heating, transportation, oil, cement and brick industries, dust storms, agriculture fires, and domestic and public generators. The results showed that the pollution levels in several sites exceeded the national and international standards. Air pollution concentrations in four Iraqi cities were recorded and analyzed in Ref. [2]. Also, the impact of these concentrations on public health and air quality was evaluated. It was found that the CO and NO2 levels were less than the World Health Organization (WHO) air quality standards in the studied cities. The main air quality index influencers were PM2.5 and PM10 concentrations. The highest pollution concentration levels were in Baghdad and Al-Muthanna. Ref. [16] assessed the heavy elements, i.e., Hg, Cd, Zn, As, Cu, Ni, and Co, concentrations in the Shwan Refinery, Kirkuk Governorate, and surrounding areas' surface

soil. The heavy elements were analyzed using 20 soil samples in various soil fractions. The results revealed high concentrations in the clay fraction; Hg was an exception where it concentrated in the coarse sandy fraction. The geo-accumulation index (Igeo) revealed high Ni and Co pollution levels and low Hg, Cd, Cu, and Zn pollution levels. These pollution levels were impacted by wind and petroleum products transportation routes. The present investigation studies air pollution dispersion from its source employing the Gaussian plume model. The present study focuses on understanding how pollutants spread in the surrounding areas and assessing their impact. The research considers factors such as pollutant type, wind speed, and wind direction to analyze their influence on dispersion patterns.

2.STUDY AREA

Kirkuk City is an ancient city whose origins date back to 1,600 years B.C. Originally built as a castle on a circular hill, it is situated amidst the Zagros Mountain, the minor Zab and Tigris rivers, and the Hamren Mountain series. The city is renowned for its shrines, mosques, and historical ruins, some dating back to the early third millennium B.C. Kirkuk's strategic location has also contributed to its significance as a commercial hub. Administratively, it serves as the center of Kirkuk Governorate. Astronomically, Kirkuk lies between (35° 31' 20" N) and (35° 20' 20" S) and the two longitudinal circles of (44° 26' 10" E) and (44° 16' 30" W) [17]. The area of the city is approximately 5023 km². The city is located 350 m above sea level [18]. The weather is characterized as hot, semi-arid, very hot, and dry in summer and cold in winter [19].

3.METHODOLOGY

3.1.Study Area Description and Point Sources Selection

The present study focuses on the model of air pollution dispersion from point sources using the Gaussian plume model. The case study area selected for this investigation is Kirkuk, a city in Iraq (Fig. 1). Kirkuk is a significant industrial center surrounded by various areas, i.e., industrial, residential, and urban. The population in Kirkuk is around one million [17,21]. The city is home to the Kirkuk oil refinery, a key industrial facility that contributes significantly to producing and processing petroleum products. The refinery complex includes several units and facilities: catalytic cracking units, crude oil distillation units, and storage facilities. The Kirkuk oil refinery is one of the region's main point sources of air pollution. The complex emits different pollutants, such as sulfur dioxide, nitrogen oxides, particulate matter, and volatile organic compounds. Kirkuk City and its refinery were selected as a case study because of their high population and industrial activities, presenting an excellent dispersion model to analyze. The present investigation aims to enhance the understanding of air pollution dispersion from its point sources and develop effective mitigation strategies to enhance industrialized urban sites' air quality.

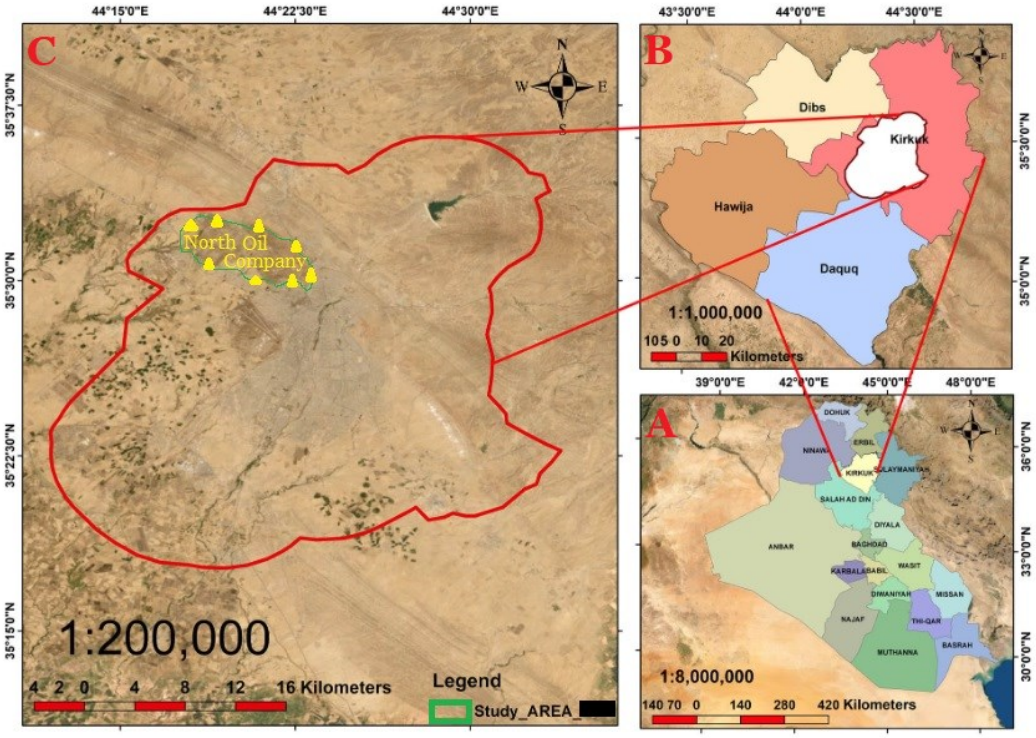

Fig. 1 (A) A Map of Iraq that Marked the Location of Kirkuk Governorate in Yellow, (B) A Map of Districts of Kirkuk Governorate, and (C) An Image of the City of Kirkuk with the Red Border and the Study Area of the North Oil Company by the Green Border with the Samples Taken in Yellow. [20].

3.2.Collecting Data and Acquisition

3.2.1.Meteorological data

The wind directions in Kirkuk City-Iraq for the period (2014-2021) are listed in Table 1. The dominant wind directions are Northwest (NW) and Southwest (SE), frequently accruing monthly and annually. The southeast (SE) and northwest (NW) winds dominate at the year's beginning, end, and middle. East (E), North (N), and Northeast (NE) occur occasionally in certain months or years. These wind patterns highlight the significance of considering the wind direction to assess the air quality in the studied area. The monthly wind speeds in the studied area for (2014-2021) are shown in Fig. 2. The wind speeds ranged from (0-2.5) m/s, i.e., relatively slow because most speeds range from 1.0 to 2.0 m/s. Although the wind speed fluctuated throughout different periods, insignificant trends and inconsistent patterns appeared. The Kirkuk City's air temperatures for (2014-2021) are presented in Fig. 3. The measured temperatures were between 9 °C and 39 °C. During the year, Kirkuk City is exposed to a temperature range, i.e., the highest in July and August. The peak temperatures were 37 °C and 39 °C. The lowest temperatures can be observed in December, January, and February, ranging from 9 °C to 14 °C. In other words, Kirkuk City witnesses a temperature variation through different months. However, Kirkuk City faces a typical continental climate, i.e., hot summer and relatively mild winter. Kirkuk City's relative humidity is from 20% to 82%, as presented in Fig. 4. Throughout a year, Kirkuk City witnesses variable levels of relative humidity, i.e., the highest (55% to 82%) in December, January, and February and the lowest (19% to 30%) in June, July, and August. The meteorological data in Table 1 and Figs. 2 to 4 were obtained from [Iraqi Meteorological Organization 2023; Unpublished Data].

Table 1 Wind Directions (°) in Kirkuk City, Iraq (2014-2021) Iraqi Meteorological Organization.

Year	Jan.	Feb.	Mar.	Apr.	May	Jun.	Jul.	Aug.	Sep.	Oct.	Nov.	Dec.
2014	↘	↘	↘	↘	↖	↖	↖	↖	↖	↖	↘	↘
2015	↘	↖	↘	↖	↖	↖	↖	↖	↖	↘	↘	↘
2016	↘	↘	↘	↘	↖	↖	↖	↖	↖	↖	→	→
2017	→/↗	→/↓	→	→	→	↖	↖	↖	↖	↖	↖	↖
2018	↓	↘	↖	↖	↖	↖	↖	↖	↖	↗	↓	↓
2019	→	↓	↓	↑	↑	↖	↖	↖	↖	↗	↗	
2020	↘	↓	↘	↗	↑	↑	↑	↖	↑	↗	↗	↖
2021	↘	↗	↗	↖	↑	↖	↖	↖	↖	↖	↗	↗

N↑, S↓, E→, NE↗, NW↖, SE↘

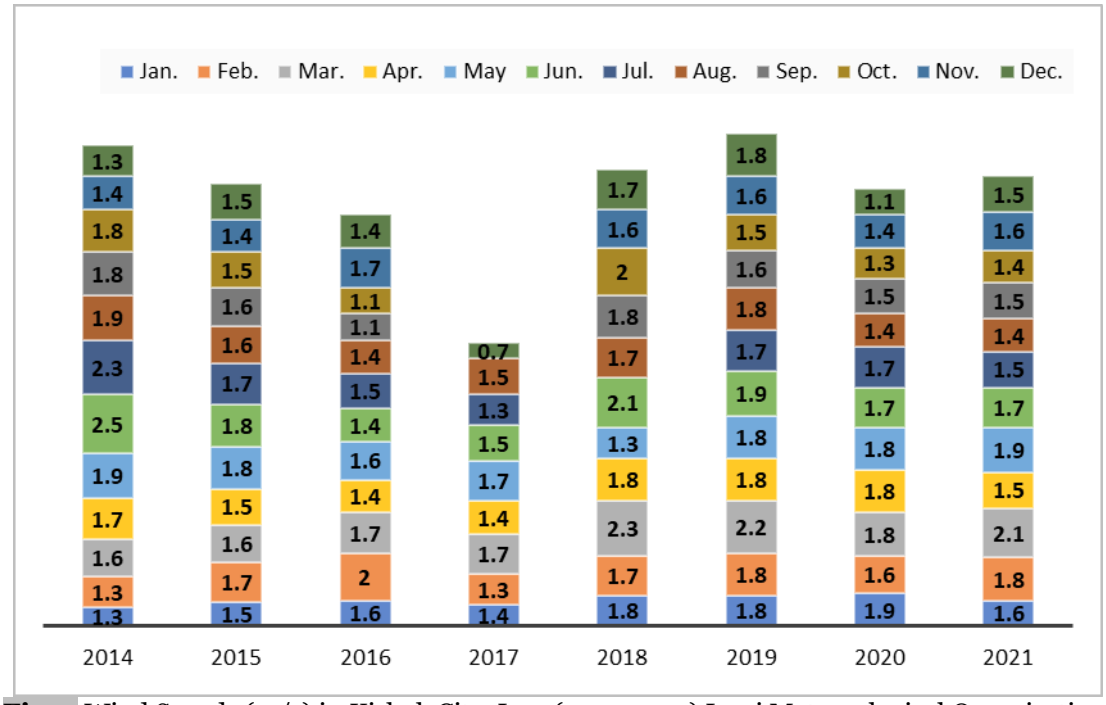

Fig. 2 Wind Speeds (m/s) in Kirkuk City, Iraq (2014-2021) Iraqi Meteorological Organization.

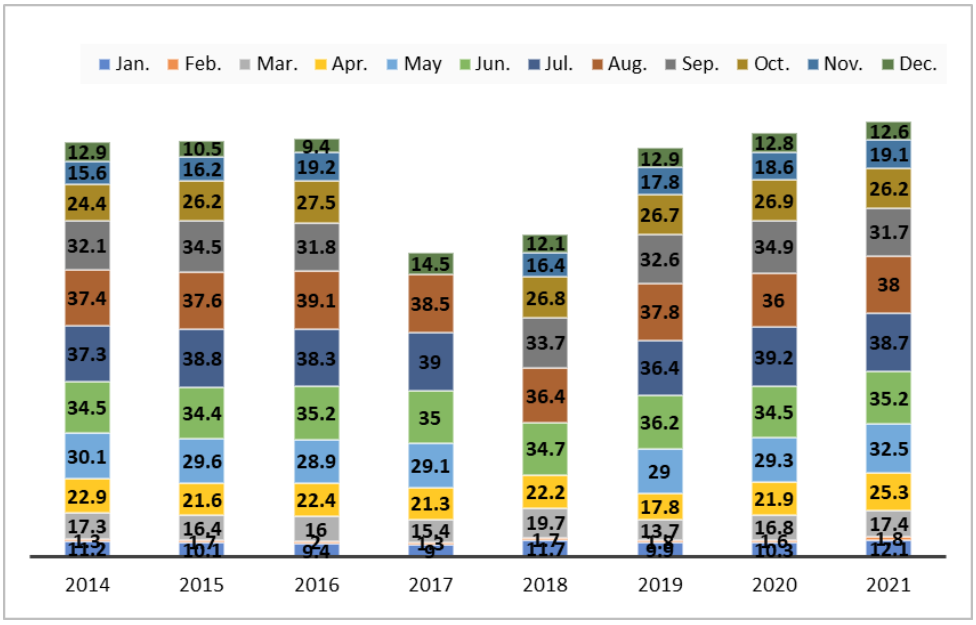

Fig. 3 Air Temperatures (°C) in Kirkuk City-Iraq (2014-2021) Iraqi Meteorological Organization.

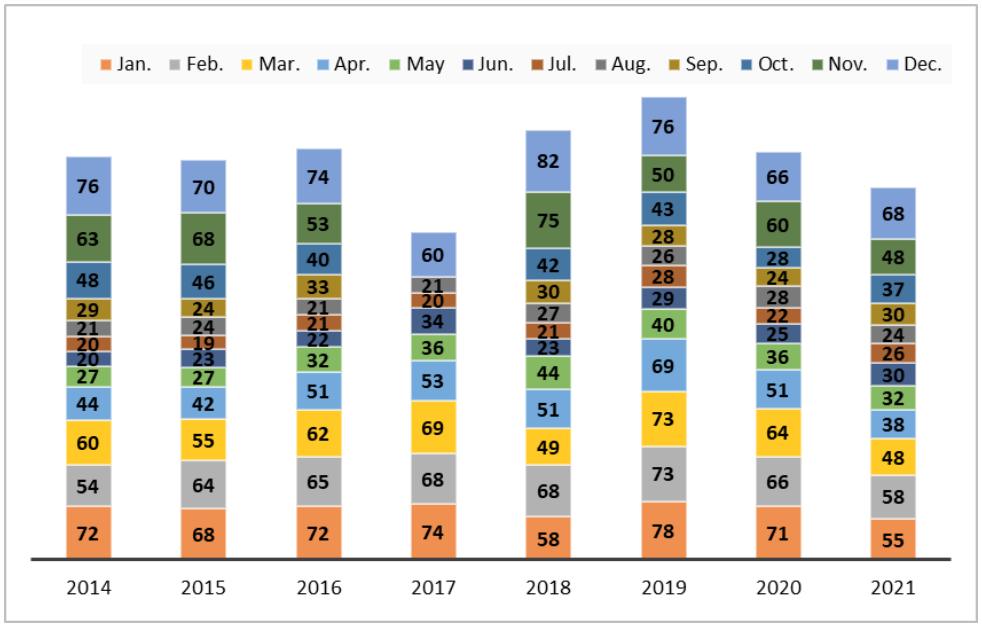

Fig. 4 Relative Humidity (%) in Kirkuk City, Iraq (2014-2021) Iraqi Meteorological Organization.

3.2.2.Source Emissions Data (Pollutant Type, Emission Rates)

This research focuses on modeling air pollution dispersion from the Kirkuk oil refinery in Kirkuk, Iraq, including CO, SO_2, NO_2, O_3, CO_2, H_2S, PM_1, $PM_{2.5}$, PM_5, and PM_{10}. Due to their impact on air quality, subsequently, human health, and the environment, such pollutants were selected. The emission data specific to the Kirkuk oil refinery were provided by the refinery operators. This data includes the emission rates of each pollutant type mentioned above. The emission rates are addressed in various units, such as (g/second) or (tpd), and are typically referred to as either average emission rates or as second/daily emissions during specific operational conditions (Table 2).

Table 2 Emission rates of various gases and pollutants from the Kirkuk oil refinery.

Pollutant	Emission rate (tons/day)/ (grams/ second)
CO*	100/ 1157.41
SO_2*	50/ 578.70
NO_2*	25/ 289.35
O_3**	10/ 115.74
CO_2*	1,000/ 11574.07
H2S*	1/ 11.57
PM1**	2/ 23.15
PM2.5**	1/ 11.57
PM5**	0.5/ 5.79
PM10**	0.25/ 2.89

* Kirkuk Oil Company
** World Health Organization

3.3.The Gaussian Plume Model: Equations and Assumptions

In atmospheric dispersion modeling, the Gaussian plume model is broadly utilized to approximate the pollutants concentration, i.e.,

emitting from a point source. It assumes many assumptions and employs certain equations to determine the concentrations of the pollutant at various heights and distances away from the point source. The pollutants concentration (C_p) can be calculated from Eq. (1) [22].

$$C_p = \frac{Q}{2\pi Du}\exp\left(-\frac{d^2}{2\sigma_y^2}\right)\left(\exp\left(-\frac{(z-H)^2}{2\sigma_z^2}\right)+\exp\left(-\frac{(z+H)^2}{2\sigma_z^2}\right)\right) = \frac{Q}{2\pi Du}\exp\left(-\frac{d^2}{2\sigma_y^2}\right)\cosh\left(\frac{zH}{\sigma_z}\right) \quad (1)$$

where C_p represents the pollutants concentration at distance d from the point source (µg/m³), Q represents the pollutants emission rate (µg/m³), D represents the dispersion coefficient (m), u represents the wind speed (m/s), z represents the measurement point height (m), H represents the plume height (m), and σ_y and σ_z represent the Gaussian distribution standard deviation in the y- and z-directions (m). Two terms form Eq. (1): (i) the exponential concentration decay with respect to distance, and (ii) the plume vertical distribution. The pollutant vertical dispersion is captured by the hyperbolic cosine function [22].

3.4.Pollutant Type Impact in the Gaussian Plume Model Analysis

Studying the influence of pollutant type in the Gaussian plume model is significant in identifying the patterns of concentration and dispersion of different atmospheric pollutants. C(x,y,z), i.e., the concentration of the pollutants at a certain time and location, is determined from Eq. (2).

$$C(x,y,z,t) = \frac{Q}{2\pi\sigma_x\sigma_y\sigma_z u}\,exp\left(-\frac{(x-x_0)^2}{2\sigma_x^2}-\frac{(y-y_0)^2}{2\sigma_y^2}-\frac{(z-z_0)^2}{2\sigma_z^2}\right) f(e) \quad (2)$$

where σ_x; $x_0, y_0, and\ z_0$; and f(e) are the Gaussian distribution standard deviation in the x-direction (m), the pollutant point source coordinates (m), and a function describing the relation between pollutant concentration and its type, respectively. It is worth pointing out that f(e) differs according to the pollutant type and depends on the physical properties of the pollutant. As for the pollutant concentration at d distance away from a point source, it can be expressed as,

$$C_p = \frac{Q}{2\pi Dd}\,exp\left[-\left(\frac{k\,d}{2}\right)^2\right] \quad (3)$$

where k is the decay coefficient (time).

The present work also studied various pollutants, such as CO, SO2, NO2, O3, CO2, H2S, and various sizes of particulate matter, i.e., PM1, PM2.5, and PM5. According to WHO, each pollutant has a symbol, description, unit, and standard limit, as listed in Table 3. Each pollutant has decay and dispersion coefficients to indicate the pollutant concentration reduction rate and the dispersion extent, as tabulated in Table 4 [23].

Table 3 Description and WHO Standard Limits for Various Pollutants [WHO].

Pollutant	Symbol	Description	Unit	WHO Standard Limit & Exposure Time
Carbon monoxide (CO)	CO	A colorless, odorless gas produced by incomplete combustion of fuels.	ppm	8 hours: 10 ppm; 1 hour: 40 ppm
Sulfur dioxide (SO_2)	SO_2	A colorless, pungent gas produced by burning fossil fuels containing sulfur.	ppm	24 hours: 10 ppm; 1 hour: 35 ppm
Nitrogen dioxide (NO_2)	NO_2	A reddish-brown gas produced by burning fossil fuels that contain nitrogen.	ppb	24 hours: 40 ppb; 1 hour: 100 ppb
Ozone (O_3)	O_3	A colorless, odorless gas is formed when sunlight reacts with pollutants in the atmosphere.	ppm	8 hours: 0.065 ppm
Carbon dioxide (CO_2)	CO_2	A colorless, odorless gas that is a natural greenhouse gas.	ppm	400 ppm
Hydrogen sulfide (H_2S)	H_2S	A colorless, flammable gas that has a rotten egg odor.	ppm	8 hours: 0.01 ppm; 1 hour: 0.1 ppm
Particulate matter (PM_1)	PM_1	Particles that are less than 1 micrometer in diameter.	µg/m³	24 hours: 25 µg/m³; 1 year: 15 µg/m³
Particulate matter ($PM_{2.5}$)	$PM_{2.5}$	Particles that are less than 2.5 micrometers in diameter.	µg/m³	24 hours: 10 µg/m³; 1 year: 5 µg/m³
Particulate matter (PM_5)	PM_5	Particles that are less than 5 micrometers in diameter.	µg/m³	24 hours: 25 µg/m³; 1 year: 15 µg/m³

Table 4 Decay and Dispersion Rates of Various Pollutants [Kirkuk Oil Company].

Pollutant	Symbol	Decay (per hour)	Dispersion (per kilometer)
Carbon monoxide	CO	0.0125	0.05
Sulfur dioxide	SO_2	0.005	0.025
Nitrogen dioxide	NO_2	0.0025	0.0125
Ozone	O_3	0.001	0.006
Carbon dioxide	CO_2	0.0005	0.003
Hydrogen sulfide	H_2S	0.00025	0.00125
Particulate matter $_1$	PM_1	0.0001	0.0006
Particulate matter $_{2.5}$	$PM_{2.5}$	0.00005	0.0003
Particulate matter $_5$	PM_5	0.000025	0.000125
Particulate matter $_{10}$	PM_{10}	0.00001	0.00006

3.5.Wind Speed and Direction Impact on Air Pollution Dispersion Assessment

Wind speed and direction impact on air pollution dispersion assessment is vital to understanding and managing air quality. The wind effect characterizes the wind impact on pollutant dispersion, as described in Eq. (4).

$$\text{wind effect} = \frac{\exp(2\sin(\theta))}{d} \quad (4)$$

where θ represents the angle difference between the wind and travel directions (°). The exponential function represents the non-linear relationship between pollutant dispersion and wind. On the other hand, the sine function represents the wind effect directional component. Combining wind speed and wind direction, the wind effect provides a significant assessment tool for assessing the pollutants' dispersion and predicting their potential effect on air quality in a studied area.

4.RESULTS AND ANALYSIS

4.1.Air Pollution Dispersion Patterns Simulated From Point Sources

The air pollution dispersion patterns simulated from point sources were studied employing the Gaussian dispersion model. The simulation commenced by generating a distance field using a grid resolution of 100 m, as shown in Fig. 5. The source point, at (439087.79, 3932262.0), represented the origin. Various parameters were studied to simulate the pollution dispersion. The wind speed and direction were 2 m/s and 174°, respectively, and the emission rate was 25 (g/s). The maximum distance was 20 km from the source point to cover the whole grid, allowing extensive dispersion patterns and their spatial distribution assessment. The modeled pollutant concentration was determined in (µg/m³). The results revealed a minimum concentration of 1.19×10^{-28} µg/m³, a maximum concentration of 11.26 µg/m³, and a mean concentration of 0.46 µg/m³, as shown in Fig. 6. These results revealed significant new information on the air spreading manner from the point source. The obtained concentration data presented a full impression of the gained pollution levels through the studied area. The minimum concentration implies less polluted areas. Meanwhile, the maximum concentration implies significantly polluted areas. The mean concentration implies averaged polluted areas.

4.2.Evaluation of the Influence of Wind Speed and Wind Direction on air Pollution Dispersion

The air pollution dispersion influence evaluation of the wind speed and wind direction was conducted utilizing the Gaussian model. The present study evaluated various wind directions (174°, 88, 235°, and 305°) impact air pollution dispersion patterns. Consistent parameter values were utilized throughout the study to perform the simulations. All pollutant masses' emission rate was grams/second. The plume height and diameter were 47 m and 8 m, respectively. The studied wind speed was 2 m/s. Figure 7 presents the simulation results evaluating the influence of wind speed and direction on air pollution dispersion employing the Gaussian model. Table 5 provides the minimum, mean, and maximum concentrations of pollutants in µg/m³ for each wind direction. The concentration values were rounded to five decimal places for enhanced precision. Across all wind directions, the minimum concentration of pollutants was consistently observed as 0.00000 µg/m³, which indicates that in large parts of the study area, especially regions that are far away from the source point, the concentration of pollutants was extremely low or negligible. The mean concentration of pollutants varied slightly with different wind directions. The mean values ranged from 0.00837 µg/m³ to 0.00856 µg/m³. These results suggested that the average pollution levels far from the source point remained relatively low regardless of the wind direction. The maximum concentration of pollutants showed variation based on wind direction. The highest maximum concentration recorded was 23.80796 µg/m³ for a wind direction of 235°. In comparison, the lowest maximum concentration was 9.28569 µg/m³ for a wind direction of 174°, indicating that specific wind directions increased the pollutants concentrations in certain areas downwind from the point source.The results revealed that the wind direction significantly impacted the air pollution dispersion patterns. The differences in the observed maximum concentrations in different wind directions ensure that wind patterns were considered as air pollution dispersion was assessed. Different wind directions caused different pollutant distribution patterns, impacting the concentration levels in different regions. The concentration level variation for various wind directions assured the significance of considering such factors in air pollution mitigation strategies and management.

Table 5 Air Pollution Dispersion Results for Different Wind Directions.

Wind Direction	Minimum Concentration (µg/m³)	Mean Concentration (µg/m³)	Maximum Concentration (µg/m³)
174°	0	0.0084	9.28569
88°	0	0.0084	12.4377
115°	0	0.0084	18.0083
235°	0	0.0086	23.808
305°	0	0.0084	12.1441

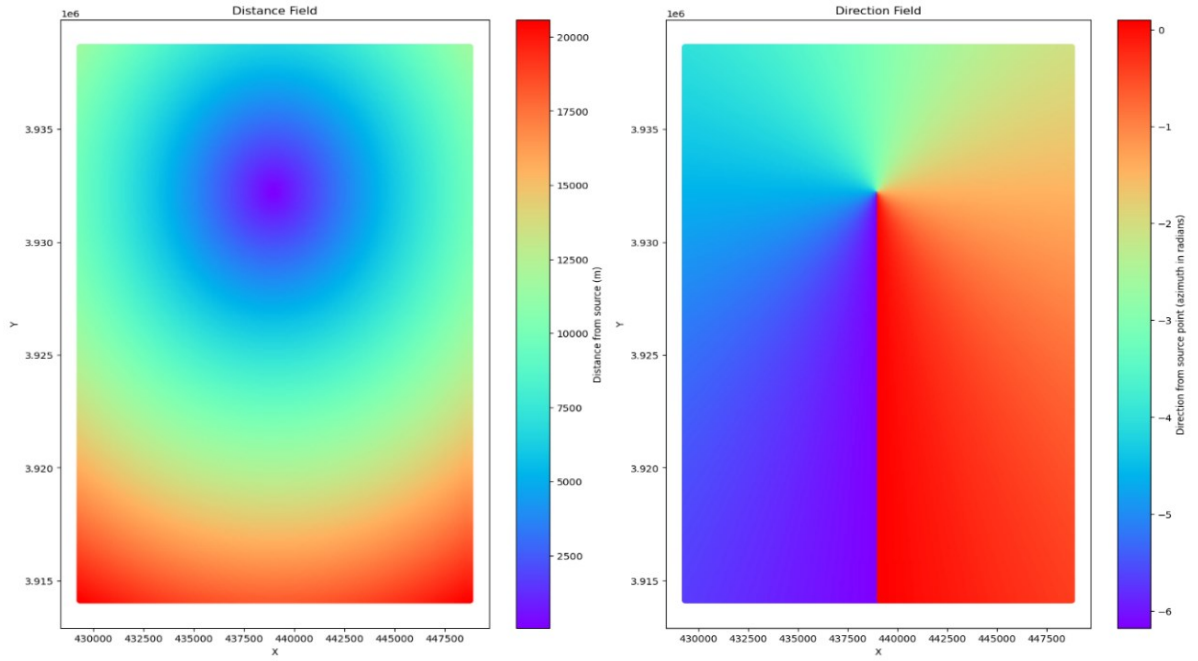

Fig. 5 Distance and Direction Fields Calculated Based on the Designed Grid and the Pollution Source Point (439087.79, 3932262.0).

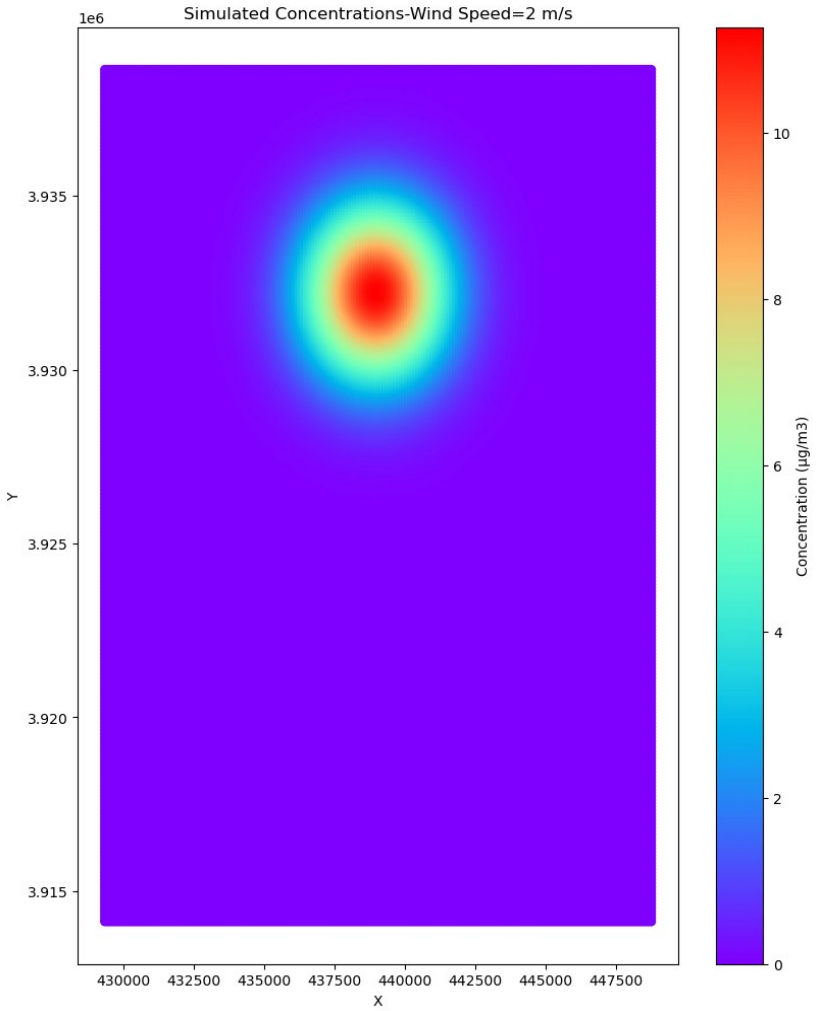

Fig. 6 Simulated Pollutant Dispersion at Ground Level (2 m) from the Source Point According to the Gaussian Dispersion Model at 2 m/s.

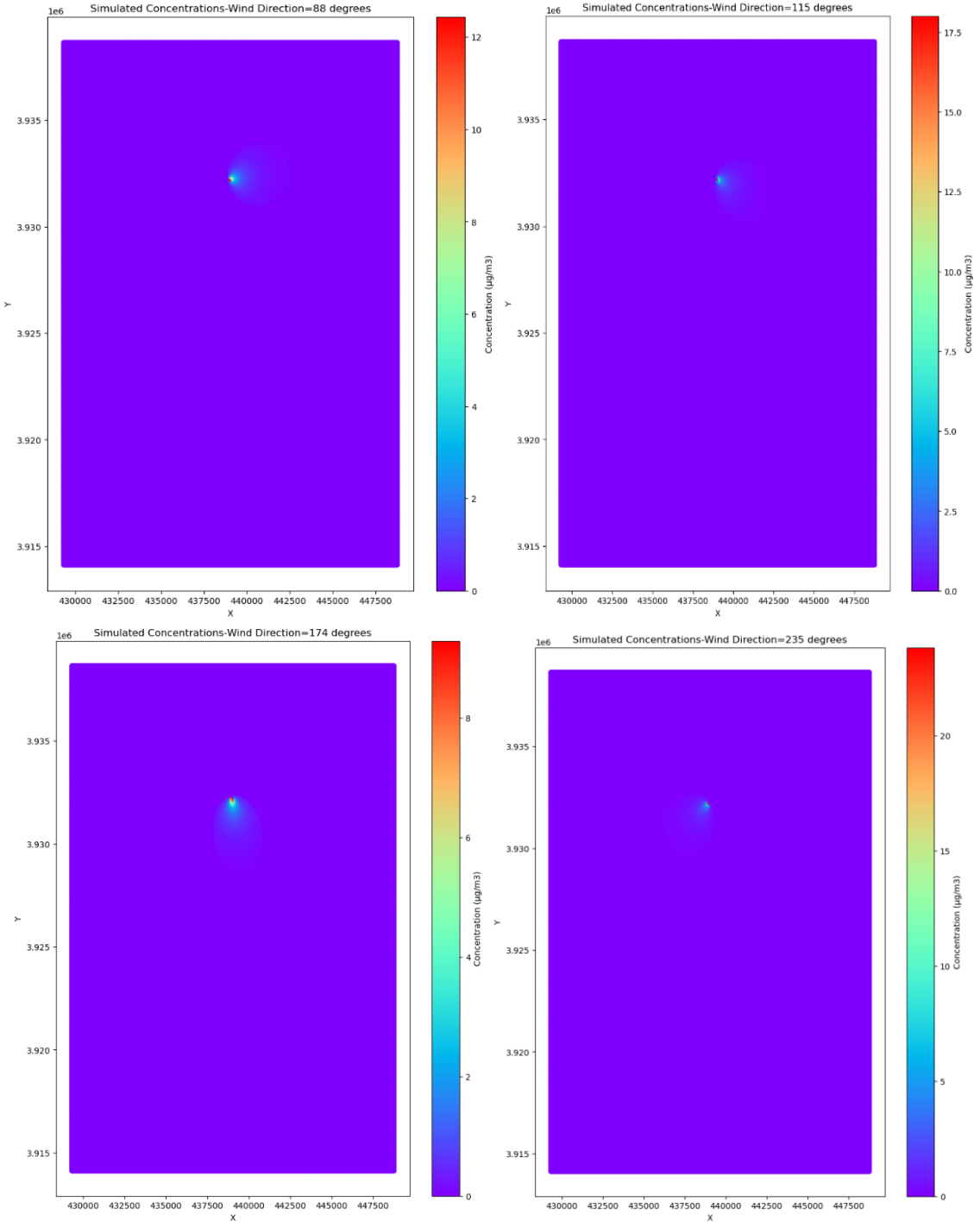
Simulated Concentrations-Wind Direction=88 degrees
Simulated Concentrations-Wind Direction=115 degrees
Simulated Concentrations-Wind Direction=174 degrees
Simulated Concentrations-Wind Direction=235 degrees
1e6
X
Y
Concentration (µg/m3)

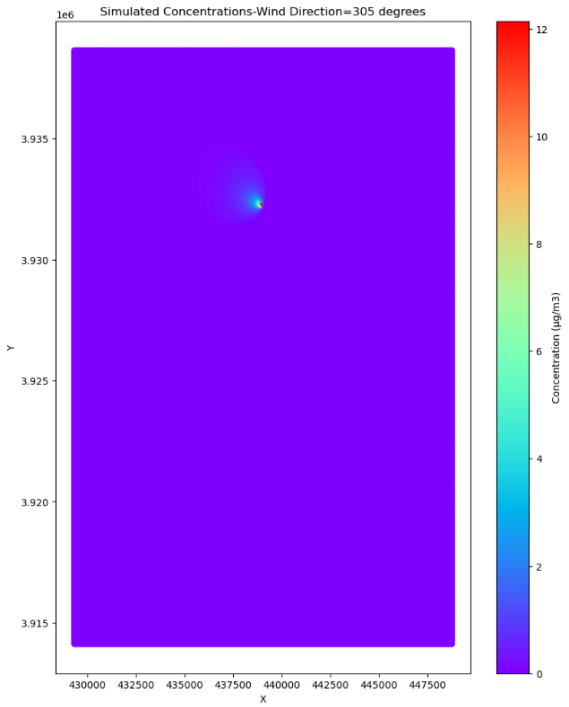

Fig. 7 Modeled Pollutant Dispersion at Ground Level (2 m) from the Source, According to the Gaussian Dispersion Model at Various Wind Directions.

4.3.Pollutant Type Impact on Dispersion Patterns Analysis

The pollutant type impacts dispersion patterns analysis by employing simulated air pollution maps generated from a point source. The studied factors were wind direction (174°), wind speed (2 m/s), plume height (47 m), and plume diameter (8 m). The data showed that each pollutant's dispersion characteristic is expressed by its decay and dispersion coefficients. CO, SO_2, NO_2, O_3, CO_2, H_2S, and various particulate matter fractions, i.e., PM_1, $PM_{2.5}$, PM_5, and PM_{10}, were considered in the present analysis. Such coefficients highlighted the pollutants' behavior in the atmosphere and their inclination to scatter through space. Each pollutant emission rate was considered to evaluate the dispersion patterns. The modeled air pollution dispersion maps offered a visual representation of the pollutants' spatial spread from the source point, as shown in Fig. 8. Analyzing these maps enables observation of the dispersion patterns and understanding of the pollutant type impact on the pollutant spatial distribution. The dispersion patterns are impacted by many factors, such as wind direction and speed, emission rates, and the pollutants' physical properties. The analysis results showed the pollutant dispersion complex nature. Various pollutant types showed different dispersion patterns because of their physical properties and emission rate variations. For instance, gases, such as CO and SO_2, inclined to rapidly disperse because of their relatively high dispersion and decay coefficients. Whereas particulate matter particles inclined to show more localized dispersion patterns because of their large particle sizes and low dispersion coefficients.

Table 6 presents concentration values of various pollutants, including CO, SO_2, NO_2, O_3, CO_2, H_2S, PM_1, $PM_{2.5}$, PM_5, and PM_{10}. The concentrations were tabulated with five-digit precision. Detailed information regarding the minimum, mean, and maximum data is reported. Table 6 shows that the minimum concentration found for the studied pollutants was 0.00000, indicating unpolluted areas due to dispersion, dilution, or the absence of emission sources. The mean concentration data highlights each pollutant's average pollution levels. Remarkably, the highest mean concentration was for CO2 (5.32149 µg/m³) and then CO (0.51779 µg/m³), suggesting that these two pollutants had higher mean levels than others. Examining the maximum concentration data reveals that CO2 had the highest concentration compared to others (6734.62380 µg/m³), which is significantly higher than the maximum values for other pollutants. It indicates that CO_2 concentrations can reach alarming levels in certain areas or under specific emission conditions. The variation in concentration levels among the different pollutants reflects their sources, chemical properties, and dispersion characteristics. For example, gases like CO, SO_2, and NO_2 showed relatively higher concentrations than particulate matter (PM) pollutants, such as PM_1, $PM_{2.5}$, PM_5, and PM_{10}, which can be attributed to the different emission sources and behavior of gases and particulate matter in the atmosphere.

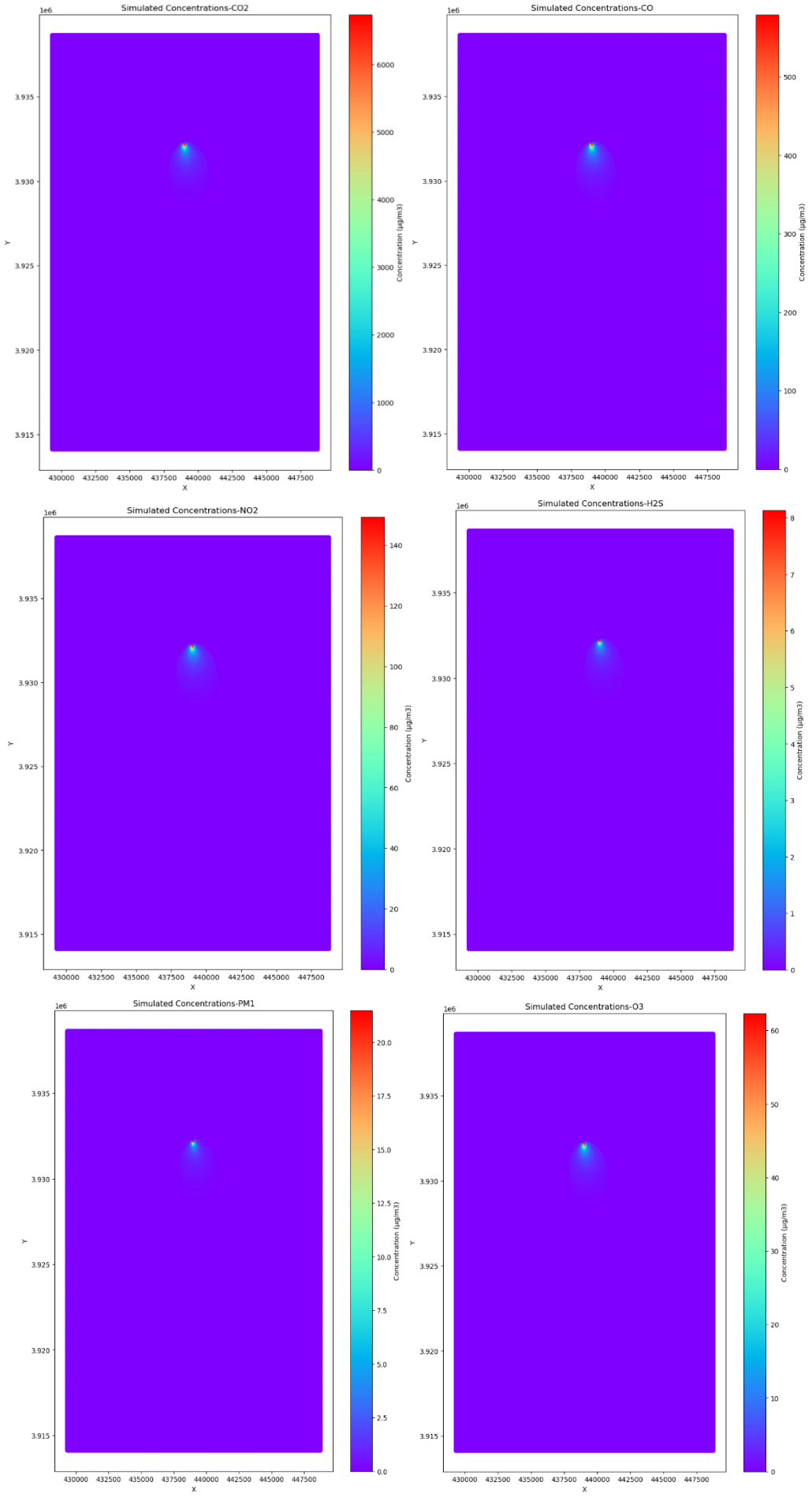
Simulated Concentrations-CO2
Simulated Concentrations-CO
Simulated Concentrations-NO2
Simulated Concentrations-H2S
Simulated Concentrations-PM1
Simulated Concentrations-O3
1e6
X
Y
Concentration (µg/m3)

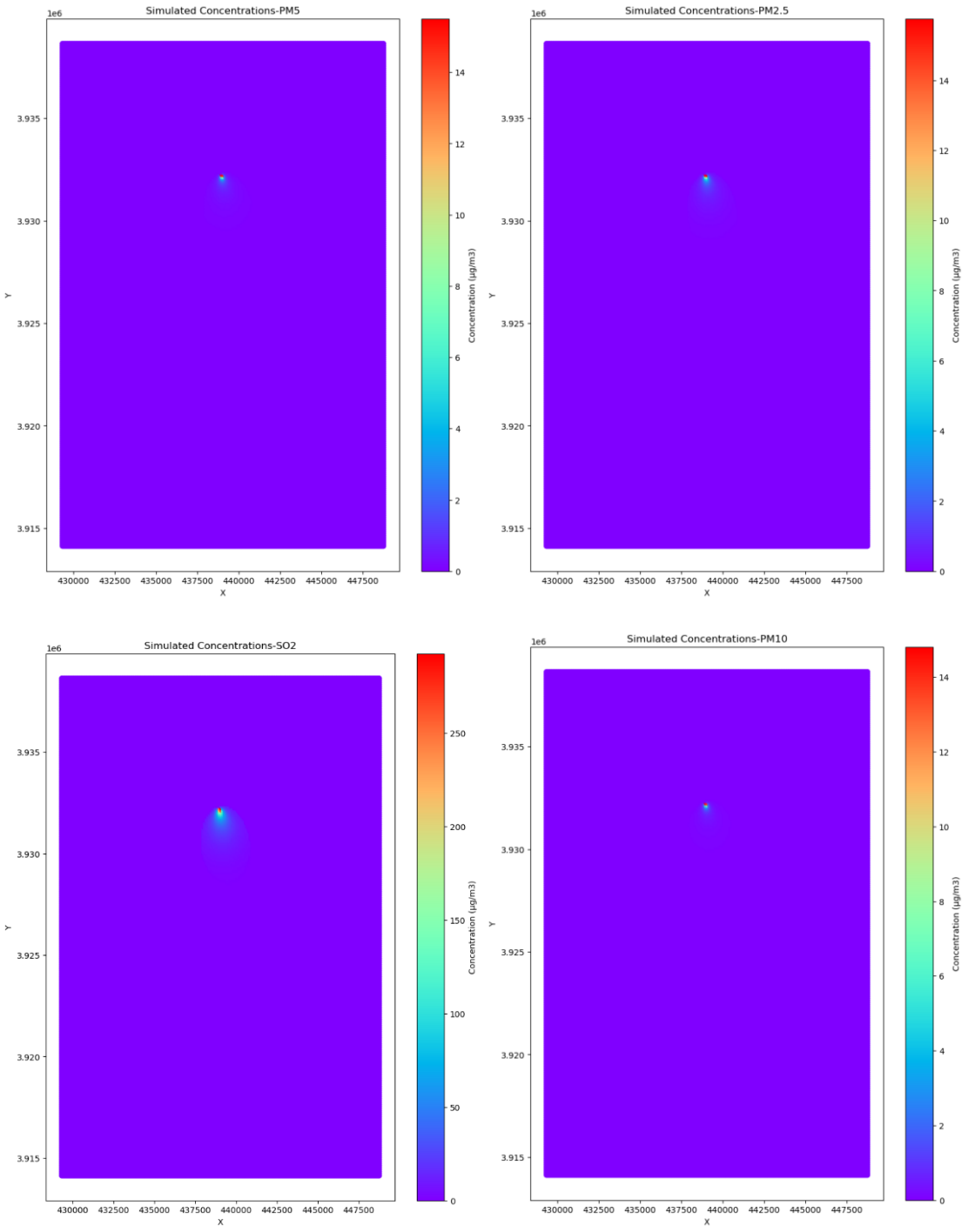

Fig. 8 Pollutant Dispersion from the Source Point According to the Gaussian Dispersion Model with Various Pollutant Types.

Table 6 Summary of Minimum, Mean, and Maximum Concentration Values for Different Pollutants. The Concentrations Were Simulated at the Ground Level at 2 Meters Height.

Pollutant	Min	Mean	Max
CO	0	0.5178	579.2081
SO_2	0	0.2594	292.6097
NO_2	0	0.1301	149.313
O_3	0	0.0525	62.33226
CO_2	0	5.3215	6734.624
H_2S	0	0.0055	8.13557
PM_1	0	0.0119	21.49274
$PM_{2.5}$	0	0.0067	15.75357
PM_5	0	0.0044	15.50106
PM_{10}	0	0.0032	14.80893

The results were compared with an air pollution monitoring study conducted in 2005 at the North Oil Company for some elements [24]. It was found that the wind speed and direction significantly impacted the pollutant transfer. The gases (H2S, CO2, CO, O3) that were compared are considered the most important and most harmful to humans, as they were all close to the study in this paper and did not exceed the internationally permissible limit.

5.CONCLUSION

This research investigated the influence of pollutant type, wind speed, and wind direction on air pollution dispersion patterns utilizing the Gaussian plume model. The present study's main results showed dispersion patterns and concentration levels for various pollutant types. The highest calculated mean and maximum concentrations were for CO, indicating its inclination to scatter over long distances. The particulate matter fractions experienced various concentration levels. PM1 had higher mean and maximum concentration levels than other particulate matter fractions. Wind speed and direction significantly influence dispersion patterns. Various wind directions caused various concentration distributions. In light of the present results, many future works and model improvements can be suggested. First, pollutant emissions' spatial and temporal variations can be further investigated to accurately capture the pollution sources' heterogeneity, which will refine emission rate input data for the dispersion models and improve their capabilities to predict. Also, utilizing more meteorological data, such as atmospheric stability and turbulence, may increase the precision of the dispersion forecast. In addition, studying additional pollutant sources and geographic regions could expand understanding of the air pollution dispersion dynamics. Regarding enhancing the present model, the Gaussian plume model limitations and uncertainties should be addressed. Also, considering non-steady-state conditions and utilizing real-time meteorological data may improve the model's pertinence to dynamic atmospheric conditions. Finally, the interaction between various pollutants and their chemical transformations can be considered in the model to provide a more comprehensive and realistic air pollution dispersion evaluation.

ACKNOWLEDGEMENTS

The authors are grateful to everyone who provided them with moral support and assistance to avoid difficulties completing this paper.

FUNDING

This research received no specific financing from funding organizations in the public, corporate, or not-for-profit sectors.

DECLARATION OF COMPETING INTEREST

The authors confirm that they have no known financial or interpersonal conflicts that could have influenced the research provided in this article.

REFERENCES

[1] Saleh SAH, Mohamed GH, Mohamed Z B. **Air Quality Index (AQI) for Kirkuk City.** *Kirkuk University Journal-Scientific Studies* 2016; **11**(1): 185-201.

[2] Abbas TR, Abbas RR. **Assessing Health Impact of Air Pollutants in Five Iraqi Cities Using AirQ+ Model**. *1st International Conference on Sustainable Engineering and Technology 2020 December 15-16*; Baghdad, Iraq: p. 012006.

[3] Khan S, Hassan Q. **Review of Developments in Air Quality Modelling and Air Quality Dispersion Models**. *Journal of Environmental Engineering and Science* 2020; **16**(1): 1-10.

[4] Moharreri MA, Arkian F, Lari K, Salehi GR. **PM_{10} and CO Dispersion Modeling of Emissions from Four Thermal Power Plants in Mashhad, Iran.** *Scientia Iranica* 2020; **27**(5): 2433-2442.

[5] Saleh SH, Hassoon AF. **Atmospheric Stability Classes and its Effect on co-Concentration Emission Around Kirkuk Refinery**. *2nd International Conference on Physics and Applied Sciences 2021 May 26-27*; Baghdad, Iraq. Mustansiriyah University: P. 012034.

[6] Atamaleki A, Zarandi SM, Fakhri Y, Mehrizi EA, Hesam G, Faramarzi M, Darbandi M. **Estimation of Air Pollutants Emission (PM_{10}, CO, SO_2 and NO_x) During Development of the Industry Using AUSTAL 2000 Model: A New Method for Sustainable Development**. *MethodsX* 2019; **6**: 1581-1590.

[7] Modi M, SK LA, Hussain Z. **A Review on Theoretical Air Pollutants Dispersion Models**. *International Journal of Pharmaceutical, Chemical & Biological Sciences* 2013; **3**(4): 1224-1230.

[8] Matacchiera F, Manes C, Beaven RP, Rees-White TC, Boano F, Mønster J, Scheutz C. **AERMOD as a Gaussian Dispersion Model for Planning Tracer Gas Dispersion Tests for Landfill Methane Emission Quantification**. *Waste Management* 2019; **87**: 924-936.

[9] Munir S, Mayfield M, Coca D, Mihaylova LS, Osammor O. **Analysis of Air Pollution in Urban Areas with Airviro Dispersion Model—A Case**

Study in the City of Sheffield, United Kingdom. *Atmosphere* 2020; **11**(3): 285, (1-27).

[10] Yang Z, Yao Q, Buser MD, Alfieri JG, Li H, Torrents A, Hapeman CJ. **Modification and Validation of the Gaussian Plume Model (GPM) to Predict Ammonia and Particulate Matter Dispersion**. *Atmospheric Pollution Research* 2020; **11**(7): 1063-1072.

[11] Anad AM, Hassoon AF, Al-Jiboori MH. **Assessment of Air Pollution Around Durra Refinery (Baghdad) from Emission NO_2 Gas at April Month**. *Baghdad Science Journal* 2022; **19**(3): 515-527.

[12] Masih A. **Machine Learning Algorithms in Air Quality Modeling**. *Global Journal of Environmental Science and Management* 2019; **5**(4): 515-534.

[13] Abdullah EJ, Mohammed MS. **Survey of Air Quality and Health Risk Assessment Around East Baghdad Oil Field, Iraq**. *Diyala Journal for Pure Science* 2021; **17**(03): 25-42.

[14] Tiwari A, Kumar P, Baldauf R, Zhang KM, Pilla F, Di Sabatino S, Pulvirenti B. **Considerations for Evaluating Green Infrastructure Impacts in Microscale and Macroscale Air Pollution Dispersion Models**. *Science of The Total Environment* 2019; **672**: 410-426.

[15] Al-Kasser MK. **Air Pollution in Iraq Sources and Effects**. *1st International Virtual Conference on Environment & Natural Resources 2021 March 24-25*; Al-Diwaniyah, Iraq. University of Al-Qadisiyah: p. 012014.

[16] Al-Teay SY, Al-Jumaily HA. **Environmental Impact Assessment of Heavy Metals Pollution in the Surface Soil Surrounding the Shwan Private Oil Refinery, Northeastern Kirkuk**. *The Iraqi Geological Journal* 2023; **56**(1D): 67-80.

[17] Hasan SF, Shareef MA, Hassan ND. **Speckle Filtering Impact on Land Use/Land Cover Classification Area Using the Combination of Sentinel-1A and Sentinel-2B — A Case Study of Kirkuk City, Iraq**. *Arabian Journal of Geosciences* 2021; **14**(4): 276.

[18] Al-jaf AFO, Al-ameen JA. **Comparison of a Traditional Landfill and a Mechanically-Biologically Treated waste Landfill (Case study; Kirkuk landfill)**. *Tikrit Journal of Engineering Sciences* 2021; **28**(2): 73-79.

[19] Hadi AM, Mohammed AK, Jumaah HJ, Ameen MH, Kalantar B, Rizeei HM, Al-Sharify ZTA. **GIS-Based Rainfall Analysis Using Remotely Sensed Data in Kirkuk Province, Iraq: Rainfall Analysis.** *Tikrit Journal of Engineering Sciences* 2022; **29**(4): 48-55.

[20] Raheem AM, Omar NQ, Naser IJ, Ibrahim MO. **GIS Implementation and Statistical Analysis for Significant Characteristics of Kirkuk Soil**. *Journal of the Mechanical Behavior of Materials* 2022; **31**(1): 691-700.

[21] Shareef MA, Hassan ND, Hasan SF, Khenchaf A. **Integration of Sentinel-1A and Sentinel-2B Data for Land Use and Land Cover Mapping of the Kirkuk Governorate, Iraq**. *International Journal of Geoinformatics* 2020; **16**(3): 87-96.

[22] Snoun H, Krichen M, Chérif H. **A Comprehensive Review of Gaussian Atm-Ospheric Dispersion Models: Current Usage and Future Perspectives**. *Euro - Mediterranean Journal for Environmental Integration* 2023; **8**(1): 219–242.

[23] Zhu H, Liu X, Wang Q, Sun J. **The Simulation of Release Consequence with A Modified Gaussian Plume Model**. In: Harada K, Matsuyama K, Himoto K, Nakamura Y, Wakatsuki K. (eds). Fire Science and Technology 2015: *10th Asia-Oceania Symposium on Fire Science and Technology 2017*: 445-454.

[24] Al-Abdraba WMS. **Study of Air Pollution Resulting from the North Oil Company in Kirkuk**. Ph. D. Thesis. College of Engineering University of Mosul. Mosul, Iraq; 2005 (in Arabic)).